Brain oscillations track the formation of episodic memories in the real world

Griffiths, Benjamin; Debener, Stephan; Mazaheri, Ali; Hanslmayr, Simon

DOI:
10.1016/j.neuroimage.2016.09.021

Document Version
Peer reviewed version

Citation for published version (Harvard):
Griffiths, B, Debener, S, Mazaheri, A & Hanslmayr, S 2016, 'Brain oscillations track the formation of episodic memories in the real world', *NeuroImage*, vol. 143, pp. 256-266.
https://doi.org/10.1016/j.neuroimage.2016.09.021

Brain oscillations track the formation of episodic memories in the real world

Benjamin Griffiths[1], Ali Mazaheri[1], Stefan Debener[2], Simon Hanslmayr[1]

1. School of Psychology, University of Birmingham, Birmingham, United Kingdom
2. Department of Psychology, Carl von Ossietzky University Oldenburg, Oldenburg, Germany

Contact Information / Corresponding Authors

Benjamin Griffiths

b.j.griffiths.1@pgr.bham.ac.uk

Simon Hanslmayr

s.hanslmayr@bham.ac.uk

+44 121 4146203

Abstract

Despite the well-known influence of environmental context on episodic memory, little has been done to increase contextual richness within the lab. This leaves a blind spot lingering over the neuronal correlates of episodic memory formation in day-to-day life. To address this, we presented participants with a series of words to memorise along a pre-designated route across campus while a mobile EEG system acquired ongoing neural activity. Replicating lab-based subsequent memory effects (SMEs), we identified significant low to mid frequency power decreases (<30Hz), including beta power decreases over the left inferior frontal gyrus. When investigating the oscillatory correlates of temporal and spatial context binding, we found that items strongly bound to spatial context exhibited significantly greater theta power decreases than items strongly bound to temporal context. These findings expand upon lab-based studies by demonstrating the influence of real world contextual factors that underpin memory formation.

Keywords: episodic memory; context; oscillations; mobile electroencephalography

Introduction

Episodic memory refers to rich memories of personally experienced events. The details of these memories not only encompass the event itself but also the surrounding environmental setting, such as where and when the event occurred. Environmental context change can have a profound effect on episodic memory (Godden and Baddeley, 1975; Smith and Vela, 2001). Yet despite such context change being typical in day-to-day life, these changes are rarely incorporated in neuroscientific experiments examining episodic memory (often due to the need to conduct these experiments in magnetic resonance imaging [MRI] or magnetoencephalogram [MEG] suites). In these experiments, it is possible that mechanisms relating to the encoding of environmental context are supressed, as context remains largely consistent and therefore irrelevant to the task. This means that the neural correlates of episodic memory observed in the lab may provide an incomplete picture of episodic memory in the real world. While it is impossible to implement MEG or MRI in daily-life settings, progress has been made in the use of portable EEG outdoors (De Vos et al., 2014; Debener et al., 2012). Embracing these advances, we aimed to investigate the influence of vibrant real world environments on the electrophysiological correlates of episodic memory formation.

One of the most common approaches to studying episodic memory formation is the subsequent memory effect (SME). SMEs are the neural signature of successful memory formation, calculated by contrasting the neural activity at encoding which predicts later remembering with the activity that predicts later forgetting, hence isolating the activity unique to memory formation. Oscillatory SMEs are in part characterised by alpha and beta (8-12Hz; 13-30Hz) power decreases (Burke et al., 2015a; Fellner et al., 2013; Greenberg et al., 2015; Guderian et al., 2009; Hanslmayr et al., 2009;

Meeuwissen et al., 2011; Noh et al., 2014; Weiss and Rappelsberger, 2000). Additionally, theta has often been implicated in memory formation, although discrepancies exist in the literature with both theta power increases and decreases purported to underlie successful memory formation (Burke et al., 2015a, 2013; Fell et al., 2011; Guderian et al., 2009; Merkow et al., 2014; Noh et al., 2014; Nyhus and Curran, 2010; Staudigl and Hanslmayr, 2013). Nevertheless, beta power (13-20Hz) decreases have been shown to reliably arise over task-relevant sensory regions during successful memory formation, a result attributed to information processing (Hanslmayr et al., 2012). Critically, a recent EEG-repetitive transcranial magnetic stimulation (rTMS) study has demonstrated that beta power decreases are causally relevant to this process (Hanslmayr et al., 2014). The predictability of these beta power decreases provide a reliable benchmark to contrast with real world recordings in order to identify whether the typical lab-based SME is observable in a real world environment.

Beyond the validation of previous lab-based findings, portable EEG technology allows the investigation of aspects of episodic memory that only occur in their entirety in the real world, such as item-to-context binding. Item-to-context binding can be assessed via contextual clustering - a behavioural phenomenon in which several events are recalled together based on contextual similarities they share. Contextual clustering has often been demonstrated for events which share a similar temporal context (i.e. events that occurred at similar points in time; Howard & Kahana, 2002). However, contextual clustering is not solely restricted to the time domain (e.g. Long, Danoff, & Kahana, 2015; Polyn, Norman, & Kahana, 2009). Of particular relevance here, studies have also demonstrated spatial contextual clustering where events that occurred in similar locations are recalled together (Copara et al., 2014; Miller, Lazarus, Polyn, & Kahana, 2013). To date, this phenomenon is predominantly studied in virtual reality where participants navigate low-resolution environments with limited visuospatial information. Vestibular and locomotion cues are distinctly lacking in many virtual reality experiments, yet lesion studies in rats have shown that these cues have been shown to have a profound impact on spatial navigation (Stackman and Herbert, 2002; Wallace et al., 2002). The absence of such cues may impede the development of a comprehensive spatial contextual representation.

It is also worth noting that a number of studies investigating spatial context have relied on random travel patterns to dissociate spatial and temporal contextual effects. A large number of random trajectories would inevitably mean that spatial and temporal context incidentally coincide at various points during the experiment, introducing a confounding variable and potentially trivial explanation of spatial clustering. In our experiment, we aimed to overcome this issue by using novel navigational paths that allow the observation of the independent contributions of temporal and spatial context to episodic memory formation.

On an oscillatory level, Long and Kahana (2015) demonstrated that temporal clustering correlates with gamma power increases in the left inferior frontal gyrus and the hippocampus during encoding. However, to the best of our knowledge, no other experiment has further investigated the relationship between neural oscillations at encoding and contextual clustering. Therefore, it remains unknown whether these patterns of activation are unique to subsequent temporal clustering or a part of a more general associative mechanism. If the former is true, then the oscillatory correlates of item-to-spatial context binding also remain unknown. *A priori* assumptions follow that subsequent temporal and spatial clustering would encompass the medial temporal lobe (MTL) – the home of place and time cells (Eichenbaum, 2014; MacDonald et al., 2011; O'Keefe, 1976). Given the intimate relationship between place cells and theta band activity, it may also be plausible to suggest that the spatial clustering effect would be observable within the theta frequency (Burgess and O'Keefe, 2011; O'Keefe and Recce, 1993).

It is of course important to identify potential oscillatory confounds that may arise in 'real world' paradigms that are not present in lab-based experiments. Numerous mobile brain body imaging (MoBI; Makeig, Gramann, Jung, Sejnowski, & Poizner, 2009) studies have demonstrated that both event-related potentials (ERPs) and oscillatory activity can be observed in moving participants (De Sanctis et al., 2014; Gramann et al., 2010; Gwin et al., 2010; Malcolm et al., 2015; Wagner et al., 2014). However, in relation to oscillatory activity, movement-related changes in power changes across the frequency spectrum (~1Hz to 90Hz). More specifically, in comparison to standing, walking can produce alpha/beta band power suppression and gamma power increases in sensorimotor areas (Castermans et al., 2014; Seeber et al., 2015, 2014; Wagner et al., 2016, 2012), whilst a loss of balance has been linked to an increase in theta band activity (Sipp et al., 2013). Importantly, these latter findings share spectral similarities with the SME. Therefore, in order to avoid potential contamination of these effects, the EEG data obtained is this experiment was acquired solely while participants were stationary.

In this experiment, we asked two questions; 1) can oscillatory lab-based episodic memory studies be validated in real-life settings? and 2) what are the neural correlates of temporal and spatial contextual clustering? Following a predefined route and led by the experimenter (see figure 1a and 1b), participants were presented with words to encode and associate with their current location (see figure 1c), a situation similar to remembering several text messages on the way to the supermarket. Participants were shown 4 lists of 20 words, where each list was presented on a spiralling route (see figure 1a). These spiralling routes were used to help disentangle the relationship between temporal and spatial context (see methods for details). After being shown a list of words, participants were removed from the environment and completed a free recall test. Finally, participants guided the experimenter to where they thought each recalled word was shown and the

location was marked by GPS. We aimed to replicate the well-documented low to mid frequency power decreases (<30 Hz) in lab-based subsequent memory studies (e.g. Burke et al., 2015b; Hanslmayr and Staudigl, 2014), in particular the beta power decreases over the left inferior frontal gyrus elicited by verbal SME paradigms (Hanslmayr et al., 2011). Furthermore, we aimed to identify and dissociate the neural correlates of spatial and temporal contextual encoding. To this end, we contrasted neural activity associated with subsequent temporal clustering with that of subsequent spatial clustering. In short, this is the first experiment directly observing the neural correlates of episodic memory encoding in the real world, allowing both the validation of a large body of the episodic memory literature and the identification of how real world context affects the neural correlates of encoding.

Materials and Methods

Participants

29 University of Birmingham students (18-39 years, 69% female) were recruited through a participant pool and rewarded with financial compensation for participation. Nine participants were excluded from the sample due to issues in recording leading to insufficient trials (n=4), poor weather conditions leading to insufficient trials (n=2) or extreme performance in the task (recalled <15 items, or forgot <15 items across all blocks; n=3). Recording complications meant that one block was lost for 3 participants leaving only 60 trials prior to preprocessing, however as there were still a sufficient number of trials (>=15 remembered and >=15 forgotten) after artefact rejection these participants remained in the sample. All participants were native English speakers or had lived in an English speaking country for the past 5 years. Participants reported normal or corrected-to-normal vision. Our sample size boundary (n=20) matched similar studies which have produced reliable oscillatory subsequent memory effects (e.g. Hanslmayr, Spitzer, & Bauml, 2009). A power analysis on pilot behavioural data indicated that a sample size of 16 participants was adequate for detecting a significant behavioural effect (α=0.05; 1–β=0.80). Ethical approval was granted by the University of Birmingham Research Ethics Committee, complying with the Declaration of Helsinki.

Materials

80 unique abstract nouns and 80 unique locations were split into 4 blocks (20 words and locations per block). The nouns were selected from the MRC Psycholinguistic Database based on scores of low imaginability and concreteness (Coltheart, 1981). All locations within a block were found in the same large, open space on the university campus. Lists and locations were counterbalanced across participants. Words were presented in black on a light grey background using the OpenSesame experiment builder (2.9.4; Mathôt, Schreij, & Theeuwes, 2012) on a Google Nexus 7 (2013; Google, Mountain View, California) tablet running Android OS (5.1.1). Tones were elicited by the tablet and

passed onto a StimTracker (Cedrus Corporation, San Pedro, California), which in turn passed a trigger to the EEG amplifier. Within each block, the navigated route formed a spiral (although participants were unaware of this; see figure 1a). In figure 1a, the dotted red line depicts the temporal sequence in which each black dot (representing a presentation location) was visited. The distance between each of these black dots when following the temporal sequence was approximately 20m. In contrast, the distance between the black dots on neighbouring loops was approximately 10-15m. Therefore, the black dots on neighbouring loops were closer in Euclidean distance than items presented on the same loop. To exhibit large amounts of temporal clustering, participants would have to recall items on the same loop (i.e. closer in time, further in space). Conversely, to exhibit large amounts of spatial clustering, participants would have to recall items on neighbouring loops together (i.e. closer in space, further in time). This distinction helped to disentangle the effects of temporal and spatial context while keeping rehearsal time between items constant. A Garmin eTrex 30 Outdoor Handheld GPS Unit (Garmin Ltd., Canton of Schaffhausen, Switzerland) was used to navigate the route and to mark co-ordinates during the spatial memory test. The GPS could accurately pinpoint a current location to approximately within 3 metres.

Procedure

Prior to commencing the experiment, participants were informed of the experimental procedure, completed a screening questionnaire and provided informed consent. During the encoding stage of each block, the experimenter walked the participant along a spiral path and at predefined locations stopped the participant to present them with a word on the tablet screen. When they were brought to a stop, participants were asked to immediately fixate upon the tablet screen. Critically, the participant was stationary whenever a stimulus was shown, attenuating movement-related EEG artifacts that could contaminate recordings. During stimulus presentation, the experiment stood to the left and to the front of the participant to ensure the participant could clearly see the tablet without moving their head. After haptic input from the experimenter (given once the participant was stationary), a fixation cross was displayed in the centre of the screen for 2.5 to 3 seconds (uniformly random), followed by a target word presented for 3 seconds. The lengthy pre-stimulus interval ensured that any motor/motor-rebound effects would not contaminate EEG recordings during the presentation window. The participant then encoded the word and the location. We intentionally asked participants to encode location in order to demonstrate that participants could accurately recall spatial information. If, on a whole, participants were found to be unable to recall spatial information accurately, it would be dubious to suggest that such information could influence recall in such a way as to produce spatial contextual clustering. Participants' retention of spatial information did not influence spatial clustering (see results). After 20 locations had been visited, the participant completed a short subtraction distractor task ("starting at x, count down in steps of y, all the way to

zero") to disrupt any working memory effects. The participant was then walked to a testing cubicle and given 3 minutes to freely recall as many of the words presented as possible. Subsequently, the experimenter walked the participant back outside and, using the list of recalled words as a cue, the participant attempted to return to where each word was presented. GPS co-ordinates for each of these recalled locations were recorded. After the participant had recalled as many of the locations as they could remember, the experimenter walked them to the next area in order to start the following block.

Behavioural Analysis

Spatial accuracy of recalled locations was determined by calculating the distance between the presentation and recalled locations of each word using the Haversine formula (which corrects for the curvature of the earth), providing a parametric measure of accuracy in metres. To assess spatial and temporal clustering, we used a variation on previous methods (Kahana, 1996) to assess the extent to which a recalled item was influenced by the previously recalled items. This variation allows the direct comparison of temporal and spatial clustering, expanding upon earlier studies which have used separate methods to analyse temporal and spatial clusters (Miller, Lazarus, et al., 2013). An error term was used to identify whether participants recalled in spatial and/or temporal clusters. 'Contextual error' describes the extent to which an individual deviated from the immediate context when recalling events; the smaller the contextual error, the less they deviated from the immediate context and therefore the greater the contextual clustering. Contextual error was derived using the equation below:

$$\textit{Contextual Error} = ((|\textit{Observed Lag}_{n,n-1}| - \textit{Expected Lag}_{n,n-1}) + (|\textit{Observed Lag}_{n,n-2}| - \textit{Expected Lag}_{n,n-2})) / 2$$

Here, *n* refers to the recalled item under observation, *n-1* to the item recalled immediately before *n*, and *n-2* to the item recalled immediately before *n-1*. $\textit{Observed Lag}_{n,n-1}$ refers to the contextual distance between the items *n* and *n-1* at encoding. Spatial contextual distance was measured in metres, while temporal distance was measured by serial lag. As each item within a block was presented approximately 25 seconds after its prior, serial lag and temporal lag are viewed as synonymous. $\textit{Expected. Lag}_{n,n-1}$ refers to the distance between item *n* and the most proximal item to *n* during encoding. $\textit{Expected. Lag}_{n,n-2}$ refers to the distance between item *n* and the second most proximal item to *n* during encoding. Subtracting the expected lag from the observed lag provides a 'raw' contextual error score ranging from zero upwards, where zero indicates perfect contextual clustering during recall and any value greater than zero indicates imperfect clustering during recall. To contrast the two modalities of context, raw contextual error scores were z-transformed using the means and standard deviations of noise data. Noise data were generated by taking the observed hits, randomly assigning a recall position to them, and then calculating the contextual error. This

provides a 'z-transformed' contextual error score where zero indicates contextual clustering observed due to chance, and any value less than zero indicating contextual clustering greater than chance. To provide a measure of clustering rather than idiosyncratic jumps between individual items, an average lag was calculated using the two previously recalled items. This method is not expected to fundamentally change the results of previous lab-based studies; Lohnas & Kahana (2014) have demonstrated that temporal clustering in free recall is influenced by multiple recent recall items, not only the immediately preceding item. One-sample t-tests were used to examine whether participants recalled in clusters more greatly than expected by chance. A dependent-samples t-test then compared temporal and spatial contextual error scores.

EEG Acquisition, Pre-processing and Time-Frequency Decomposition

EEG was recorded using a portable 'EEGo Sports' EEG system (ANT Neuro, Enschede, Netherlands) with 65 Ag/AgCl electrodes arranged in a 10/10 system layout (including left and right mastoids, CPz as reference and AFz as ground). Impedances were kept below 20 kΩ, and the sampling rate was set to 500Hz. To facilitate source analysis, head coordinates of all electrodes and the nasion, left pre-auricular area and right pre-auricular area of each participant were taken using a Polhemus Fasttrack system (Polhemus, Colchester, VT) before commencing the experiment.

The data was pre-processed using the FieldTrip toolbox (Oostenveld et al., 2011). The continuous data were epoched into single trials beginning 2000ms before word presentation and ending 3000ms after word presentation. During this time window, the participant was stationary with their eyes fixated upon the tablet screen. The data was first high-passed filtered (1Hz; Butterworth IIR) and then eye-blinks, saccades and any other consistent muscular artefacts were removed using independent component analysis. Subsequently, residual irregular artefacts were removed by rejecting the corresponding trials; mean number of trials rejected = 15.45; mean number of hits remaining = 35.25 (max: 51, min. 22); mean number of misses remaining; 26.30 (max. = 42; min. = 16). Artefact rejection was blind (i.e. the experimenter had no clue as to which trials belonged to which condition), yet peculiarly this led to a larger number of misses being rejected than hits. Speculatively, this may be a result of distraction; participants may have moved in response to one of the many numerous distractors in real world environments (e.g. unexpected loud noises). These physical movements would produce large artefacts in the EEG (much greater than the underlying brain signals) that must be rejected. Critically, such movement would also prevent the participant from attending to the word, leading to poorer memory performance for these trials. The mean number of trials rejected and included sum to 77 because 3 participants only had 60 trials worth of data at artefact rejection, making the mean number of trials completed 77 prior to artefact rejection. Bad channels were interpolated based on the data of neighbouring electrodes and the data was given an average reference (mean interpolated = 0.6; max. = 5; min. = 0).

Several previous studies indicate that electrophysiological data obtained from mobile participants is subject to more noise than their lab-based equivalents. (Castermans et al., 2014; Gwin et al., 2010; Kline et al., 2015; Snyder et al., 2015; Wagner et al., 2012). To provide an indication of the cleanliness of the data obtained here, the P300 component elicited by stimulus onset can be seen in figure 2a. The P300 component was obtained by using ICA to remove non-brain related components from the raw data and then applying a low-pass filter (15Hz). Each trial was corrected using a pre-stimulus baseline window ranging from -200ms to 0ms, Further examples of 'real world' ERPs have been demonstrated by De Vos et al. (2014) and Debener et al. (2012). In addition, a topography of this ERP is presented in figure 2b, and a time frequency representation of the data averaged over all trials time-locked to stimulus onset is presented in figure 2c.

Time-frequency analysis was conducted on the pre-processed dataset for each participant using 7 cycle Morlet wavelets for frequencies of 3 to 30Hz in 1hz steps; the time window was too short to effectively signals below 3Hz. Time was epoched from -1 to 2 seconds, where 0 seconds represents stimulus onset. Power was calculated at 50ms intervals within this window. For each frequency-channel pair, the data were z-transformed by first obtaining the average power over time for each trial, and then calculating the average and standard deviation of this time-averaged power across trials. This twice-averaged power was then subtracted from the observed power at each channel-frequency pair, and the output was divided by the standard deviation of the time-averaged power. Gaussian smoothing (2Hz, 200ms kernel) was then applied to the time-frequency representation to help reduce the impact of inter-individual differences in oscillatory response across time and frequencies.

Subsequent Memory Analysis

Trials were split into two categories; items where both word and location were later remembered (hits) and items where the word was later forgotten (misses). Note that as spatial memory was only test for words that were remembered, there was no location-remembered, word-forgotten condition. The data was first restricted to 0-1000ms post-stimulus between 15 and 20Hz to replicate previous beta power decreases seen in subsequent memory paradigms (for review, see Hanslmayr et al., 2012). Hits and misses for this time-frequency window were contrasted using a dependent samples t-test. A Monte-Carlo randomisation procedure using 2000 permutations was employed to correct for multiple comparisons (see Maris & Oostenveld, 2007). The clusters used in this randomisation procedure were defined by summing the t-values of individual channel-frequency-time triplets that exceeded threshold ($\alpha = 0.05$).

Subsequently, further power changes in the time-frequency representation were examined. Following previous literature, alpha and beta power decreases were tested, while undirected theta

power differences were tested. Accordingly, alpha and beta tests were one-tailed, while theta power tests were two-tailed. As the non-parametric cluster analysis technique only informs us as to whether there is a significant effect between conditions within the window of interest, we used a sliding window analysis (Staudigl and Hanslmayr, 2013) to enhance the temporal and spectral specificity of our overarching SME. The sliding window (200ms by 1Hz in size, 75% overlap) was passed over the time-frequency window (-1000 to 2000ms), contrasting power differences between hits and misses within the window. In this technique, the Monte-Carlo randomisation procedure alone is not sufficient to control for multiple comparisons so the p-values for each sliding window were pooled together and thresholded using false discovery rate (FDR; Benjamini & Hochberg, 1995).

Subsequent Clustering Analysis

To assess the oscillatory correlates of temporal and spatial clustering during encoding, contextual error scores were correlated with the time-frequency power spectrum. For each participant and for each time-frequency-channel point, the contextual error score for each trial was correlated with the observed power for that trial using a Spearman's Rank procedure. As less contextual error denotes greater contextual clustering, a negative r-value would indicate a power increase accompanying greater contextual clustering. To aid comprehension, each returned r-value underwent a switching of sign (+0.5 became -0.5; -0.5 became +0.5), meaning a positive r-value indicated a power increase with greater contextual clustering. The time-frequency representation of r-values was tested against the null hypothesis that there would be no correlation between power and contextual clustering. This null hypothesis was realised by creating a 'null data structure' with the same dimensions as the observed data, but with all observed data points substituted with zeros (i.e. no correlation). The observed data was then contrasted with the 'null data' in the same manner as the sliding window approach described above.

Source Analysis

Observed effects on sensor level were reconstructed in source space using individual head models in combination with the standard MRI and boundary element model (BEM) provided in the FieldTrip toolbox. The Linearly Constrained Minimum Variance (LCMV) beamformer was used to localise sources of significant activity (van Veen et al., 1997). Pre-processed data was time-locked and then shifted to source space. This placed the time-locked data onto virtual electrodes, which then underwent an identical analytical procedure to its sensor-level counterparts. P-values are presented with each source reconstruction for completeness, but as the time-frequency windows were selected because they exceeded the significance threshold on sensor level, caution should be taken when interpreting source-level p-values. These p-values were derived from a cluster-based

permutation (Maris & Oostenveld, 2007) across the whole window of interest, as defined by sensor-level analysis. Peak differences in activity were first deduced by sliding a spherical searchlight with a 6mm radius over all voxels within the interpolated significant cluster (interpolated grid size: 181x217x181mm). All voxels that fell within the sphere were summed, and the group of voxels with the largest absolute value was selected as the region of peak difference. As this approach cannot effectively handle sparse regions of activity, a follow-up visual inspection was conducted. For visual inspection, only the 1% of voxels with the most extreme t-values was examined. The results of visual inspection are only reported when they produced notable differences to the peak sphere approach.

Additional Analyses

Several further analyses were conducted but were subject to a number of analytical issues. For transparency, these analyses are listed here, but to avoid misinterpretation of the outcomes of these analyses by those glancing over the paper, these results are not reported in the results section. Theta phase to gamma amplitude coupling was investigated using the method described by Jiang, Bahramisharif, van Gerven, and Jensen (2015) in an attempt to find similar cross-frequency coupling contextual effects to those reported by Staudigl & Hanslmayr (2013). However, no differences were found, possibly due to the overly noisy gamma activity. Furthermore, differences in source-level connectivity between the medial temporal lobe and the prefrontal cortex for high versus low contextually clustered items was investigated to test the hypothesised neural context model put forward by Polyn & Kahana (2008). Unfortunately, the difference in phase angles between virtual electrode connections were almost solely clustered around 0 and π, preventing any meaningful connectivity analysis (Cohen, 2015).

Results

Behavioural Results

On average, participants recalled 50.45% of each 20 word list and when attempting to locate where each word was presented, were on average 14.74 metres away from the presentation location. Eighty percent of participants showed less temporal contextual error (i.e. more temporal contextual clustering) than spatial contextual error (see figure 3). A one-sample t-test revealed significantly greater spatial clustering than expected by chance, $t(19)=-5.728$, $p<0.001$, 95% CI [-2.155, -1.001], matching previous virtual reality results (Miller, Lazarus, et al., 2013). Furthermore, another one-sample t-test revealed significantly greater temporal clustering than expected by chance, $t(19)=-6.105$, $p<0.001$, 95% CI [-4.003, -1.959], again conforming to earlier findings (e.g. Kahana, 1996). A dependent samples t-test revealed significantly greater temporal clustering than spatial clustering, $t(19)=-3.921$, $p<0.001$, 95% CI [-2.152, -0.654]. To examine how contextual error relates to memory performance, the mean contextual error of each participant was correlated with their

average hit-rate and spatial accuracy. Temporal contextual error did not correlate with memory performance in the free recall task (r=-0.274, p=0.242) or spatial accuracy when returning to presentation locations (r=-0.237, p = 0.315); the same was true for spatial contextual error (free recall performance: r=-0.235, p=0.319; spatial accuracy: r=-0.282, p=0.229).

Subsequent Memory Analysis

Given the robust nature of lower beta power decreases over relevant sensory regions during memory formation, we first aimed to replicate a key lab-based finding in verbal episodic memory studies: a lower beta power (15-20Hz) decrease over the left inferior frontal gyrus within 1 second of stimulus onset (for review, see Hanslmayr et al., 2012). Using a cluster-based permutation test to control for multiple comparisons across all sensors (see Maris & Oostenveld, 2007), a one-tailed dependent samples t-test revealed a significant power decrease for hits in comparison to misses between 0 and 1 second post stimulus (p=0.009; see figure 4a and 4b). To identify whether this lower beta power decrease arose in the left inferior frontal gyrus, the window was then reconstructed on source level, undergoing the same analytical procedure as its sensor level counterpart. A one-tailed dependent samples t-test revealed a significant power decrease for hits in comparison to misses (p=0.026). We determined peak activity by sliding a spherical searchlight with a radius of 6mm across the significant cluster and calculating the sum of activity within this sphere (see methods for details); these results were confirmed by visual inspection of the 1% of most extreme voxels within the major cluster. Peak differences in activity between later remembered and later forgotten items were localised to left superior and middle temporal poles, [MNI coord. x=-40, y=19, z=-30; ~BA 38], while visual inspection of the most extreme 1% of voxels within the significant cluster revealed a further difference between later remembered and later forgotten items in the left inferior frontal gyrus (IFG), [MNI coord. x=-39, y=30, z=-18; ~BA 47], (see figure 4c). These results replicate the previous findings of lower beta power decreases over the left IFG following successful memory formation of verbal information (Hanslmayr et al., 2011, 2009).

Subsequently, a more comprehensive picture of the low-frequency SMEs was sought out using a sliding window analysis (see methods for details; Staudigl & Hanslmayr, 2013). Given the prevalent power decreases within the alpha and beta bands accompanying successful memory formation (Hanslmayr et al., 2012), one-tailed dependent samples t-tests were used to analyse the subsequent memory effect between 8 and 30 Hz. As some controversy surrounds theta band activity, two-tailed dependent samples t-tests where used for frequencies between 3 and 7 Hz. Analysis revealed significant, FDR corrected, p-values (p_{corr}<0.05) across the frequency and time spectrum (see figure 5). Specifically, low frequency theta (3-4Hz, p_{corr}<0.05) power decreases for hits in comparison to misses were observed between 600ms and 1200ms post-stimulus; alpha (8-12Hz, p_{corr}<0.05) power decreases for hits in comparison to misses were observed between 400ms and 800ms post-stimulus;

and beta (21-25Hz) power decreases for hits in comparison to misses were observed just before (-250ms to 0ms, $p_{corr}<0.05$) and later after stimulus onset (1000 to 1300ms, $p_{corr}<0.05$). These low frequency power decreases match many other effects reported in the literature (see Hanslmayr & Staudigl, 2014). It is worth noting that given the relatively short time window and the use of 7 cycle wavelets, any frequency below 3Hz could not be convolved. Therefore, a broadband delta/theta effect cannot be ruled out. It is also worth noting that the broadband appearance of the spectrogram is not likely due to a subsequent memory ERP, which has been shown to elicit a greater positivity following successful memory formation (e.g. Fernández et al., 1998). Rather, it may simply be due to the nature of the subsequent memory effect. For example, Burke et al., (2015b, 2014) have demonstrated broadband power decreases accompanying successful memory formation. The difference in power between subsequently remembered versus forgotten items did not correlate with spatial accuracy.

Significant regions of activity observed on sensor-level were then reconstructed on source level. Theta power decreases (3-4Hz, 600-1200ms, p=0.005) peaked in the right superior occipital area, the right precuneus and the right cuneus, [MNI coord. x=19, y=-87, z=39; ~BA 19]. Visual inspection of the theta source activity also revealed peak differences in activity within the left middle and inferior temporal gyri, [MNI coord. x=-52, y=-10, z=-26; ~BA 20], and the right superior parietal lobe, [MNI coord. x=25, y=-64, z=53; ~BA 7] (see figure 5c). Generally speaking, these theta power decreases occurred in regions associated the processing of with task-relevant stimuli (i.e. semantic processing, Pobric, Lambon Ralph, & Jefferies, 2009; Visser, Jefferies, & Lambon Ralph, 2010; visuospatial processing, Formisano et al., 2002; Sack et al., 2002), conforming to earlier findings (Greenberg et al., 2015). Alpha power decreases (8-12Hz, 500-800ms, p=0.005) peaked in the right inferior frontal gyrus, the right superior and middle temporal poles and the right insula, [MNI coord. x=40, y=19, z=-27; ~BA 38]. Post-stimulus beta power decreases (21-25Hz, 1000-1300ms, p=0.003) peaked in the left inferior frontal gyrus, left superior temporal pole and gyrus, and the left rolandic operculum, [MNI coord. x=-58, y=8, z=0; ~BA 48]. Pre-stimulus beta activity (21-25Hz, -250-200ms, p=0.003) could not be effectively localised using the spherical cluster, but visual search of the source revealed notable differences in the right superior parietal lobe and right postcentral gyrus, [MNI coord. x=27, -50, 58; ~BA 7]. In summary, the real world SME observed here appears to match what is regularly reported in lab-based studies (e.g. Greenberg et al., 2015; Hanslmayr et al., 2009).

Subsequent Clustering Analysis

Our subsequent clustering analysis was conducted on a time-frequency representation of r-values obtained from correlating the power for each channel-frequency-time data point of each trial by the clustering score of the same trial. As a first step, we examined whether the correlation between power and temporal/spatial clustering differed significantly from the null hypothesis (i.e. no

correlation; r = 0). Concerning temporal clustering, the sensor level analysis (conducted as in *Subsequent Memory Analysis*) revealed no cluster exceeding the significance threshold. This is consistent with a previous study which also found no correlation between temporal clustering and low frequency power (Long & Kahana, 2015). Concerning spatial clustering however, a sliding window analysis revealed a cluster consisting of extended slow theta power decreases across the stimulus interval (3-4Hz; -1000-1000ms, $p_{corr}<0.05$), and a broader theta post-stimulus power decrease (3-6Hz; 400-900ms, $p_{corr}<0.05$), which predicted greater spatial clustering (see figure 6). In other words, these theta power decreases were associated with a greater likelihood of recalling items that were spatially proximate to one another. As above, these windows were reconstructed in source space. The post-stimulus theta power decreases (3-6Hz; 400-900ms, $p_{corr}<0.05$) peaked in the left calcarine sulcus, cuneus and superior occipital regions, [MNI coord. x=-8, y=-97, z=20; ~BA 17] (see figure 5B). Meanwhile, the peri-stimulus theta power decreases (3-4Hz; -1000-1000ms, $p_{corr}<0.05$), peaked in left superior and medial frontal gyrus, [MNI coord. x=-8, y=39, z=51; ~BA 8] (not pictured due to strong similarity with fig. 6c).

In a second step, we contrasted the r-values obtained by correlating theta power and temporal clustering with r-values obtained by correlating theta power and spatial clustering, in order to identify whether these theta power decreases were unique to the spatial clustering condition. Cluster analysis indicated that there was a small but significant difference between temporal clustering - theta power effects and spatial clustering - theta power effects ($p_{corr}<0.05$; see figure 7a). T-values indicate that theta power decreases correlate more strongly with spatial clustering than with temporal clustering. When reconstructing this difference on source level (see figure 7b), the spatial-temporal clustering contrast (3-7Hz, 400-800ms, p=0.003) appeared to peak in left frontal superior and medial gyri, [MNI coord. x=-5, y=40, z=57; ~BA 8]. Visual inspection of the peak 1% of activity also revealed greater theta power decreases for spatial clustering from within the left medial temporal lobe, [MNI coord. x=-26, y=2, z=-35; ~BA 36].

As can be seen in figure 7b, this difference in theta power between spatial and temporal clustering occurs in a region at the boundary of the forward model and therefore may be particularly susceptible to ocular and/or muscle artifacts. To address this concern, we repeated this analysis using only the electrodes on the outer rim of the cap (FP1, FPz, FP2, AF7, AF8, F7, F8, FT7, FT8, T7, T8, TP7, TP8, P7, P8, PO7, PO8, O1, Oz, O2) as these electrodes are most likely to contain the ocular/muscle artifacts. Being able to replicate the analysis based on these electrodes alone may indicate that these findings are a result of artifacts, however the absence of a significant difference would indicate that the result is dependent on electrodes closer to cortical sources. When replicating the sensor-level spatial-temporal clustering contrast, we found no significant difference

between the two conditions over the outer rim electrodes alone. This suggests that the difference in theta power between spatial and temporal clustering was not due to ocular/muscular artifacts.

Discussion

Here, we identified the oscillatory subsequent memory effect (SME) in a real-world environment. Moreover, we examined the influence of real world contextual factors (i.e. space) on episodic memory relative to contextual factors available within the lab (i.e. time). Participants donned a portable EEG setup and were presented with verbal stimuli on a tablet across the university campus. Each list was presented on a spiral path that disentangled temporal and spatial context. Successful memory formation was accompanied by strong beta power decreases over left frontal regions for items which were later remembered in comparison to those which were later forgotten. Furthermore, a broad theta power decrease was observed shortly after stimulus presentation for items later remembered, over regions including the left temporal pole and right posterior parietal cortex. Similarly, theta power decreases accompanied strong spatial clustering within left frontal regions and the medial temporal lobe when compared to temporal clustering.

Generally speaking, our findings corroborate what others have demonstrated within a lab setting. On a behavioural level, individuals demonstrate both temporal and spatial contextual clustering in an environment where spatial details are significantly richer than what is experienced within the lab (Miller, Lazarus, et al., 2013; Miller, Neufang, et al., 2013). Expanding on previous experiments, the spiralling presentation pattern used in this experiment helped attenuate temporal and spatial contextual overlap. Knowing that temporal clustering could not inform spatial clustering and vice versa, this experiment furthers the notion that temporal clustering and spatial clustering are autonomous phenomena.

On an electrophysiological level, we replicated the established low-frequency power decreases observed during successful memory formation (Burke et al., 2015a, 2014; Fellner et al., 2013; Greenberg et al., 2015; Guderian et al., 2009; Hanslmayr et al., 2009; Meeuwissen et al., 2011; Noh et al., 2014; Weiss and Rappelsberger, 2000). Source localisation of the beta power activity revealed decreases in the left frontal and temporal pole regions, both of which are associated with verbal and semantic processing (Pobric et al., 2009). Following the information-via-desynchronisation hypothesis (Hanslmayr et al., 2012), these beta power decreases would reflect verbal information processing necessary for successful memory formation. Although discussed in previous studies (Hanslmayr et al., 2009), given the aspects of this study relating to movement we reiterate that these power decreases are not viewed as oscillatory correlates of motor activity (Salenius and Hari, 2003). The participant was stationary before and during the presentation of each stimulus, so no motor component would be systematically present during stimulus presentation. If a component relating to

motor activity did arise, then it would be evenly distributed between later remembered and later forgotten items, and hence cancel out in the later remembered-later forgotten contrast. One could still argue that a participant plans their next movement after they are confident that they have successfully encoded a stimulus before the trial has ended. Such sensorimotor planning may indeed elicit a beta power decrease (e.g. Pfurtscheller and Neuper, 1997). While we cannot rule this out based on the results of this experiment alone, this does not fit the numerous lab-based studies (e.g. Hanslmayr et al., 2011; Long and Kahana, 2015) that have found the same beta power decrease over the left inferior frontal gyrus in paradigms that have no potential for subsequent sensorimotor planning following encoding. With evidence that familiar lab-based paradigms can be replicated in real world conditions, the field can move onto more adventurous paradigms that fully embrace real world environments.

We also observed significant theta power decreases following successful memory formation, particularly for items that demonstrated strong spatial clustering at recall. These power decreases may reflect a common process – possible selective communication within and across spatially diverse regions. Diversity in phase is optimal for communication as signals can arrive at a time of peak excitability and selectively communicate with receiving, down-stream, neural assemblies (Maris et al., 2016). There is a wealth of evidence to suggest theta is well suited for such communication needs (for review, see Colgin, 2013). Critically, the diversity in theta phase beneficial for communication would be reflected by theta power decreases in regions relevant to successful memory formation, especially in macro-scopic recording techniques such as EEG. In the context of the current experiment, observed theta power decreases in the temporal poles, posterior parietal cortex and medial temporal regions likely reflect the activation of, and communication between, areas responsible for the processing of semantics (e.g. Whitney, Kirk, O'Sullivan, Lambon Ralph, & Jefferies, 2011) and spatial location (Ciaramelli et al., 2010; Miller et al., 2014). Ultimately, these oscillatory dynamics allows the formation of coherent memory episodes. This account would also explain the absence of a similar theta power decrease for temporally clustered items. Temporal clustering might rely on a smaller network involving no communication with spatial processing regions. Consistent with this assumption, a previous study linked temporal clustering to high frequency (gamma) activity which might reflect the action of more local networks (Long and Kahana, 2015).

Alternatively, the absence of a neural correlate to temporal clustering may also be a result of adapting encoding strategies across blocks. Hintzman (2016) argued that an 'intelligent' participant would favour a memory strategy that facilitates later recall, so an unsuccessful strategy in an early block may be adapted to aid performance in later blocks. Numerous memory strategies focus on memorising lists in the order they were presented (e.g. pegwords, story creation). Swapping

amongst these strategies may produce a similar degree of temporal clustering with dissimilar underlying neural correlates. That said, temporal clustering functions have been shown to remain consistent in the face of varying memory strategies and suggested to be a strategy-independent memory phenomenon (Healey and Kahana, 2014). Possibly, the absence of a clear neural correlate in this experiment was due to changes in memory strategy distorting the neural signal produced by 'true' temporal clustering.

Interestingly, we found no neural correlate of later spatial accuracy. Perhaps the short delay between the participant being stopped at the presentation location and being asked to fixate upon the screen was sufficient to process and encode the surrounding environment. Therefore, the neural activity associated with greater spatial accuracy at retrieval may have occurred prior to the defined time window of analysis. Alternatively, participants may have only begun to process the spatial location after the stimulus had disappeared from the screen. Again, this would be outside of the period of when the EEG signal was analysed. Unfortunately, as the signal outside of the planned period was contaminated with movement-related artifacts, we were unable to explore this hypothesis.

Unsurprisingly, real world EEG comes with its own challenges. Here, we will take the opportunity to discuss some of these issues in hope that this will save others from experiencing the same difficulties. Firstly, our testing was highly dependent on the weather. Even the lightest of rain could affect signal quality if the scalp were to become wet (e.g. through channel bridging). Conversely, sunny and/or humid days present the same risk as participants begin to sweat more. Secondly, the equipment setup is heavy, and due to the short cables connecting the cap to the amplifier, this weight had to be carried by the participant. Undoubtedly, this will have tired participants greatly during the experiment and may have increased sweating on the scalp, again comprising EEG signal quality. In future, this weight should be distributed as greatly as possible in order to avoid participant strain, decline in cognitive performance due to fatigue and the decline in signal quality that may accompany the strain. Finally, real world experiments most likely involve complex eye-movements as participants visually explore and process the surrounding environments. Future experiments could incorporate eye-tracking to help pinpoint the onset of neural processes (e.g. scene/object processing) and identify non-brain artifacts (e.g. macro-/micro-saccades),

In conclusion, our findings are the first to provide strong evidence for the ecological validity of lab-based experiments investigating episodic memory formation and oscillations. More importantly, our investigation into contextual clustering highlights the importance of real world memory research. We speculate that similar virtual reality studies would not observe such strong effects of spatial contextual clustering, given the lack of vestibular and locomotion cues and low-resolution visuospatial information available in virtual reality. The real world EEG approach used here can not only pave the way towards new insights into the underpinnings of contextual details in newly formed

568 memories, but also lead to realistic investigations in other domains such as spatial navigation and
569 beyond.

570 ## Acknowledgements

571 This work was supported by grants awarded to S.H. by Deutsche Forschungsgemeinschaft [Emmy
572 Noether Programme Grant HA 5622/1-1]; and the European Research Council [Consolidator Grant
573 Agreement 647954].

574 ## References

575 Benjamini, Y., Hochberg, Y., 1995. Controlling the false discovery rate: A practical and powerful
576 approach to multiple testing. J. R. Stat. Soc. Ser. B 57, 289–300.

577 Burgess, N., O'Keefe, J., 2011. Models of place and grid cell firing and theta rhythmicity. Curr. Opin.
578 Neurobiol. 21, 734–744. doi:10.1016/j.conb.2011.07.002

579 Burke, J.F., Long, N.M., Zaghloul, K.A., Sharan, A.D., Sperling, M.R., Kahana, M.J., 2014. Human
580 intracranial high-frequency activity maps episodic memory formation in space and time.
581 Neuroimage 85, 834–843. doi:10.1016/j.neuroimage.2013.06.067

582 Burke, J.F., Merkow, M.B., Jacobs, J., Kahana, M.J., Zaghloul, K.A., 2015a. Brain computer interface to
583 enhance episodic memory in human participants. Front. Hum. Neurosci. 8, 1–10.
584 doi:10.3389/fnhum.2014.01055

585 Burke, J.F., Ramayya, A.G., Kahana, M.J., 2015b. Human intracranial high-frequency activity during
586 memory processing: Neural oscillations or stochastic volatility? Curr. Opin. Neurobiol. 31,
587 104–110. doi:10.1016/j.conb.2014.09.003

588 Burke, J.F., Zaghloul, K. a., Jacobs, J., Williams, R.B., Sperling, M.R., Sharan, a. D., Kahana, M.J., 2013.
589 Synchronous and asynchronous theta and gamma activity during episodic memory formation. J.
590 Neurosci. 33, 292–304. doi:10.1523/JNEUROSCI.2057-12.2013

591 Castermans, T., Duvinage, M., Cheron, G., Dutoit, T., 2014. About the cortical origin of the low-
592 delta and high-gamma rhythms observed in EEG signals during treadmill walking. Neurosci. Lett.
593 561, 166–170. doi:10.1016/j.neulet.2013.12.059

594 Ciaramelli, E., Rosenbaum, R.S., Solcz, S., Levine, B., Moscovitch, M., 2010. Mental space travel:
595 Damage to posterior parietal cortex prevents egocentric navigation and reexperiencing of
596 remote spatial memories. J. Exp. Psychol. Learn. Mem. Cogn. 36, 619–634.
597 doi:10.1037/a0019181

598 Cohen, M.X., 2015. Effects of time lag and frequency matching on phase-based connectivity. J.
599 Neurosci. Methods 250, 137–146. doi:10.1016/j.jneumeth.2014.09.005

Colgin, L.L., 2013. Mechanisms and functions of theta rhythms. Annu. Rev. Neurosci. 36, 295–312. doi:10.1146/annurev-neuro-062012-170330

Coltheart, M., 1981. The MRC psycholinguistic database. Q. J. Exp. Psychol. 33, 497–505. doi:10.1080/14640748108400805

Copara, M.S., Hassan, A.S., Kyle, C.T., Libby, L.A., Ranganath, C., Ekstrom, A.D., 2014. Complementary roles of human hippocampal subregions during retrieval of spatiotemporal context. J. Neurosci. 34, 6834–6842. doi:10.1523/JNEUROSCI.5341-13.2014

De Sanctis, P., Butler, J.S., Malcolm, B.R., Foxe, J.J., 2014. Recalibration of inhibitory control systems during walking-related dual-task interference: A Mobile Brain-Body Imaging (MOBI) Study. Neuroimage 94, 55–64. doi:10.1016/j.neuroimage.2014.03.016

De Vos, M., Gandras, K., Debener, S., 2014. Towards a truly mobile auditory brain-computer interface: Exploring the P300 to take away. Int. J. Psychophysiol. 91, 46–53. doi:10.1016/j.ijpsycho.2013.08.010

Debener, S., Minow, F., Emkes, R., Gandras, K., de Vos, M., 2012. How about taking a low-cost, small, and wireless EEG for a walk? Psychophysiology 49, 1617–1621. doi:10.1111/j.1469-8986.2012.01471.x

Eichenbaum, H., 2014. Time cells in the hippocampus: a new dimension for mapping memories. Nat. Rev. Neurosci. 15. doi:10.1038/nrn3827

Fell, J., Ludowig, E., Staresina, B.P., Wagner, T., Kranz, T., Elger, C.E., Axmacher, N., 2011. Medial temporal theta/alpha power enhancement precedes successful memory encoding: Evidence based on intracranial EEG. J. Neurosci. 31, 5392–5397. doi:10.1523/JNEUROSCI.3668-10.2011

Fellner, M.-C., Bäuml, K.-H.T., Hanslmayr, S., 2013. Brain oscillatory subsequent memory effects differ in power and long-range synchronization between semantic and survival processing. Neuroimage 79, 361–370. doi:10.1016/j.neuroimage.2013.04.121

Fernández, G., Weyerts, H., Tendolkar, I., Smid, H.G.O.M., Scholz, M., Heinze, H.-J., 1998. Event-related potentials of verbal encoding into episodic memory: Dissociation between the effects of subsequent memory performance and distinctiveness. Psychophysiology 35, 709–720. doi:10.1111/1469-8986.3560709

Formisano, E., Linden, D.E., Di Salle, F., Trojano, L., Esposito, F., Sack, A.T., Grossi, D., Zanella, F.E., Goebel, R., 2002. Tracking the mind's image in the brain I: time-resolved fMRI during visuospatial mental imagery. Neuron 35, 185–194. doi:10.1016/S0896-6273(02)00747-X

Godden, D.R., Baddeley, A.D., 1975. Context-dependent memory in two natural environments: On land and underwater. Br. J. Psychol. 66, 325–331. doi:10.1111/j.2044-8295.1975.tb01468.x

633 Gramann, K., Gwin, J.T., Bigdely-Shamlo, N., Ferris, D.P., Makeig, S., 2010. Visual evoked responses
634 during standing and walking. Front. Hum. Neurosci. 4, 202. doi:10.3389/fnhum.2010.00202

635 Greenberg, J.A., Burke, J.F., Haque, R., Kahana, M.J., Zaghloul, K.A., 2015. Decreases in theta and
636 increases in high frequency activity underlie associative memory encoding. Neuroimage 114,
637 257–63. doi:10.1016/j.neuroimage.2015.03.077

638 Guderian, S., Schott, B.H., Richardson-Klavehn, a., Duzel, E., 2009. Medial temporal theta state
639 before an event predicts episodic encoding success in humans. Proc. Natl. Acad. Sci. 106, 5365–
640 5370. doi:10.1073/pnas.0900289106

641 Gwin, J.T., Gramann, K., Makeig, S., Ferris, D.P., 2010. Removal of movement artifact from high-
642 density EEG recorded during walking and running. J. Neurophysiol. 103, 3526–34.
643 doi:10.1152/jn.00105.2010

644 Hanslmayr, S., Matuschek, J., Fellner, M.-C., 2014. Entrainment of prefrontal beta oscillations induces
645 an endogenous echo and impairs memory formation. Curr. Biol. 24, 904–909.
646 doi:10.1016/j.cub.2014.03.007

647 Hanslmayr, S., Spitzer, B., Bauml, K.-H., 2009. Brain oscillations dissociate between semantic and
648 nonsemantic encoding of episodic memories. Cereb. Cortex 19, 1631–1640.
649 doi:10.1093/cercor/bhn197

650 Hanslmayr, S., Staudigl, T., 2014. How brain oscillations form memories--a processing based
651 perspective on oscillatory subsequent memory effects. Neuroimage 85 Pt 2, 648–655.
652 doi:10.1016/j.neuroimage.2013.05.121

653 Hanslmayr, S., Staudigl, T., Fellner, M.-C., 2012. Oscillatory power decreases and long-term memory:
654 the information via desynchronization hypothesis. Front. Hum. Neurosci. 6, 1–12.
655 doi:10.3389/fnhum.2012.00074

656 Hanslmayr, S., Volberg, G., Wimber, M., Raabe, M., Greenlee, M.W., Bauml, K.-H.T., 2011. The
657 relationship between brain oscillations and BOLD signal during memory formation: A combined
658 EEG-fMRI study. J. Neurosci. 31, 15674–15680. doi:10.1523/JNEUROSCI.3140-11.2011

659 Healey, M.K., Kahana, M.J., 2014. Is memory search governed by universal principles or idiosyncratic
660 strategies? J. Exp. Psychol. Gen. 143, 575–596. doi:10.1037/a0033715

661 Hintzman, D.L., 2016. Is memory organized by temporal contiguity? Mem. Cognit. 44, 365–375.
662 doi:10.3758/s13421-015-0573-8

663 Howard, M.W., Kahana, M.J., 2002. A distributed representation of temporal context. J. Math.
664 Psychol. 46, 269–299. doi:10.1006/jmps.2001.1388

665 Jiang, H., Bahramisharif, A., van Gerven, M. a. J., Jensen, O., 2015. Measuring directionality between

666 neuronal oscillations of different frequencies. Neuroimage 118, 359–367.
667 doi:10.1016/j.neuroimage.2015.05.044

668 Kahana, M.J., 1996. Associative retrieval processes in free recall. Mem. Cognit. 24, 103–109.
669 doi:10.3758/BF03197276

670 Kline, J.E., Huang, H.J., Snyder, K.L., Ferris, D.P., 2015. Isolating gait-related movement artifacts in
671 electroencephalography during human walking. J. Neural Eng. 12, 046022. doi:10.1088/1741-
672 2560/12/4/046022

673 Lohnas, L.J., Kahana, M.J., 2014. Compound cuing in free recall. J. Exp. Psychol. Learn. Mem. Cogn.
674 40, 12–24. doi:10.1037/a0033698

675 Long, N.M., Danoff, M.S., Kahana, M.J., 2015. Recall dynamics reveal the retrieval of emotional
676 context. Psychon. Bull. Rev. doi:10.3758/s13423-014-0791-2

677 Long, N.M., Kahana, M.J., 2015. Successful memory formation is driven by contextual encoding in the
678 core memory network. Neuroimage 119, 332–337. doi:10.1016/j.neuroimage.2015.06.073

679 MacDonald, C.J., Lepage, K.Q., Eden, U.T., Eichenbaum, H., 2011. Hippocampal "time cells" bridge
680 the gap in memory for discontiguous events. Neuron 71, 737–749.
681 doi:10.1016/j.neuron.2011.07.012

682 Makeig, S., Gramann, K., Jung, T.P., Sejnowski, T.J., Poizner, H., 2009. Linking brain, mind and
683 behavior. Int. J. Psychophysiol. 73, 95–100. doi:10.1016/j.ijpsycho.2008.11.008

684 Malcolm, B.R., Foxe, J.J., Butler, J.S., De Sanctis, P., 2015. The aging brain shows less flexible
685 reallocation of cognitive resources during dual-task walking: A mobile brain/body imaging
686 (MoBI) study. Neuroimage 117, 230–42. doi:10.1016/j.neuroimage.2015.05.028

687 Maris, E., Fries, P., van Ede, F., 2016. Diverse phase relations among neuronal rhythms and their
688 potential function. Trends Neurosci. xx, 1–14. doi:10.1016/j.tins.2015.12.004

689 Maris, E., Oostenveld, R., 2007. Nonparametric statistical testing of EEG- and MEG-data. J. Neurosci.
690 Methods 164, 177–90. doi:10.1016/j.jneumeth.2007.03.024

691 Mathôt, S., Schreij, D., Theeuwes, J., 2012. OpenSesame: an open-source, graphical experiment
692 builder for the social sciences. Behav. Res. Methods 44, 314–324. doi:10.3758/s13428-011-
693 0168-7

694 Meeuwissen, E.B., Takashima, A., Fernandez, G., Jensen, O., 2011. Evidence for human Fronto-
695 Central gamma activity during long-term memory encoding of word sequences. PLoS One 6.
696 doi:10.1371/journal.pone.0021356

697 Merkow, M.B., Burke, J.F., Stein, J.M., Kahana, M.J., 2014. Prestimulus theta in the human

698 hippocampus predicts subsequent recognition but not recall. Hippocampus 24, 1562–1569.
699 doi:10.1002/hipo.22335.Prestimulus

700 Miller, A.M.P., Vedder, L.C., Law, L.M., Smith, D.M., 2014. Cues, context, and long-term memory: the
701 role of the retrosplenial cortex in spatial cognition. Front. Hum. Neurosci. 8, 1–15.
702 doi:10.3389/fnhum.2014.00586

703 Miller, J.F., Lazarus, E.M., Polyn, S.M., Kahana, M.J., 2013a. Spatial clustering during memory search. J.
704 Exp. Psychol. Learn. Mem. Cogn. 39, 773–781. doi:10.1037/a0029684

705 Miller, J.F., Neufang, M., Solway, A., Brandt, A., Trippel, M., Mader, I., Hefft, S., Merkow, M., Polyn,
706 S.M., Jacobs, J., Kahana, M.J., Schulze-Bonhage, A., 2013b. Neural activity in human hippocampal
707 formation reveals the spatial context of retrieved memories. Science (80-.). 342, 1111–1114.
708 doi:10.1126/science.1244056

709 Noh, E., Herzmann, G., Curran, T., De Sa, V.R., 2014. Using single-trial EEG to predict and analyze
710 subsequent memory. Neuroimage 84, 712–723. doi:10.1016/j.neuroimage.2013.09.028

711 Nyhus, E., Curran, T., 2010. Functional role of gamma and theta oscillations in episodic memory.
712 Neurosci. Biobehav. Rev. 34, 1023–1035. doi:10.1016/j.neubiorev.2009.12.014

713 O'Keefe, J., 1976. Place units in the hippocampus of the freely moving rat. Exp. Neurol. 51, 78–109.
714 doi:10.1016/0014-4886(76)90055-8

715 O'Keefe, J., Recce, M.L., 1993. Phase relationship between hippocampal place units and the EEG
716 theta rhythm. Hippocampus 3, 317–330. doi:10.1002/hipo.450030307

717 Oostenveld, R., Fries, P., Maris, E., Schoffelen, J.-M., 2011. FieldTrip: Open source software for
718 advanced analysis of MEG, EEG, and invasive electrophysiological data. Comput. Intell.
719 Neurosci. 2011, 1–9. doi:10.1155/2011/156869

720 Pfurtscheller, G., Neuper, C., 1997. Motor imagery activates primary sensorimotor area in humans.
721 Neurosci. Lett. 239, 65–68. doi:10.1016/S0304-3940(97)00889-6

722 Pobric, G., Lambon Ralph, M. a., Jefferies, E., 2009. The role of the anterior temporal lobes in the
723 comprehension of concrete and abstract words: rTMS evidence. Cortex 45, 1104–1110.
724 doi:10.1016/j.cortex.2009.02.006

725 Polyn, S.M., Kahana, M.J., 2008. Memory search and the neural representation of context. Trends
726 Cogn. Sci. 12, 24–30. doi:10.1016/j.tics.2007.10.010

727 Polyn, S.M., Norman, K.A., Kahana, M.J., 2009. A context maintenance and retrieval model of
728 organizational processes in free recall. Psychol. Rev. 116, 129–156. doi:10.1037/a0014420.A

729 Sack, A.T., Sperling, J.M., Prvulovic, D., Formisano, E., Goebel, R., Di Salle, F., Dierks, T., Linden,

730 D.E.J., 2002. Tracking the mind's image in the brain II: Transcranial magnetic stimulation reveals
731 parietal asymmetry in visuospatial imagery. Neuron 35, 195–204. doi:10.1016/S0896-
732 6273(02)00745-6

733 Salenius, S., Hari, R., 2003. Synchronous cortical oscillatory activity during motor action. Curr. Opin.
734 Neurobiol. 13, 678–684. doi:10.1016/j.conb.2003.10.008

735 Seeber, M., Scherer, R., Wagner, J., Solis-Escalante, T., M??ller-Putz, G.R., 2015. High and low gamma
736 EEG oscillations in central sensorimotor areas are conversely modulated during the human gait
737 cycle. Neuroimage 112, 318–326. doi:10.1016/j.neuroimage.2015.03.045

738 Seeber, M., Scherer, R., Wagner, J., Solis-Escalante, T., Muller-Putz, G.R., 2014. EEG beta suppression
739 and low gamma modulation are different elements of human upright walking. Front. Hum.
740 Neurosci. 8, 1–9. doi:10.3389/fnhum.2014.00485

741 Sipp, A.R., Gwin, J.T., Makeig, S., Ferris, D.P., 2013. Loss of balance during balance beam walking
742 elicits a multifocal theta band electrocortical response. J. Neurophysiol. 110, 2050–60.
743 doi:10.1152/jn.00744.2012

744 Smith, S.M., Vela, E., 2001. Environmental context-dependent memory: A review and meta-analysis.
745 Psychon. Bull. Rev. 8, 203 – 220. doi:10.3758/BF03196157

746 Snyder, K.L., Kline, J.E., Huang, H.J., Ferris, D.P., 2015. Independent Component Analysis of Gait-
747 Related Movement Artifact Recorded using EEG Electrodes during Treadmill Walking. Front.
748 Hum. Neurosci. 9, 639. doi:10.3389/fnhum.2015.00639

749 Stackman, R.W., Herbert, A.M., 2002. Rats with lesions of the vestibular system require a visual
750 landmark for spatial navigation. Behav. Brain Res. 128, 27–40. doi:10.1016/S0166-
751 4328(01)00270-4

752 Staudigl, T., Hanslmayr, S., 2013. Theta oscillations at encoding mediate the context-dependent
753 nature of human episodic memory. Curr. Biol. 23, 1101–1106.

754 van Veen, B., van Drongelen, W., Yuchtman, M., Suzuki, A., 1997. Localization of brain electrical
755 activity via linearly constrained minimum variance spatial filtering. IEEE Trans. Biomed. Eng. 44,
756 867–880. doi:10.1109/10.623056

757 Visser, M., Jefferies, E., Lambon Ralph, M., 2010. Semantic processing in the anterior temporal lobes:
758 a meta-analysis of the functional neuroimaging literature. J. Cogn. Neurosci. 22, 1083–1094.
759 doi:10.1162/jocn.2009.21309

760 Wagner, J., Makeig, S., Gola, M., Neuper, C., Muller-Putz, G., 2016. Distinct Band Oscillatory
761 Networks Subserving Motor and Cognitive Control during Gait Adaptation. J. Neurosci. 36,
762 2212–2226. doi:10.1523/JNEUROSCI.3543-15.2016

763 Wagner, J., Solis-Escalante, T., Grieshofer, P., Neuper, C., Müller-Putz, G., Scherer, R., 2012. Level of
764 participation in robotic-assisted treadmill walking modulates midline sensorimotor EEG
765 rhythms in able-bodied subjects. Neuroimage 63, 1203–1211.
766 doi:10.1016/j.neuroimage.2012.08.019

767 Wagner, J., Solis-Escalante, T., Scherer, R., Neuper, C., Müller-Putz, G., 2014. It's how you get there:
768 walking down a virtual alley activates premotor and parietal areas. Front. Hum. Neurosci. 8, 93.
769 doi:10.3389/fnhum.2014.00093

770 Wallace, D.G., Hines, D.J., Pellis, S.M., Whishaw, I.Q., 2002. Vestibular information is required for
771 dead reckoning in the rat. J. Neurosci. 22, 10009–10017. doi:22/22/10009 [pii]

772 Weiss, S., Rappelsberger, P., 2000. Long-range EEG synchronization during word encoding correlates
773 with successful memory performance. Cogn. Brain Res. 9, 299–312. doi:10.1016/S0926-
774 6410(00)00011-2

775 Whitney, C., Kirk, M., O'Sullivan, J., Lambon Ralph, M. a., Jefferies, E., 2011. The neural organization
776 of semantic control: TMS evidence for a distributed network in left inferior frontal and
777 posterior middle temporal gyrus. Cereb. Cortex 21, 1066–1075. doi:10.1093/cercor/bhq180

778

779

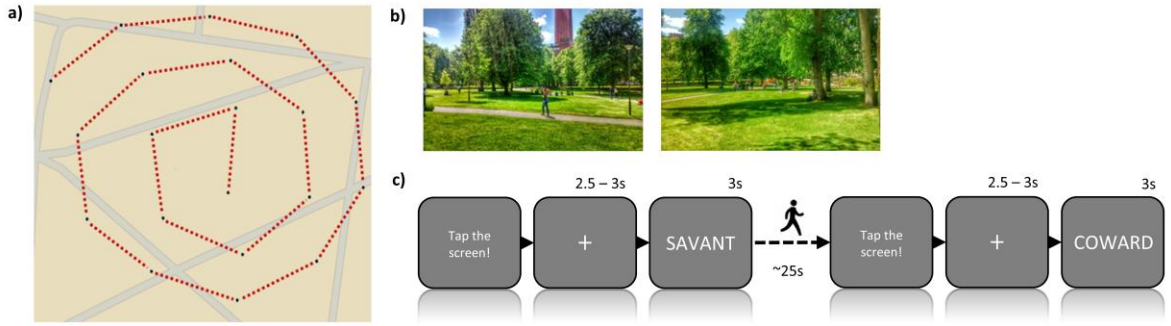

780

781 Figure 1. Behavioural paradigm. a) Spiral path. Participants were guided along the red line by the experimenter. At each
782 black dot, the participant was shown one word to encode along with the presentation location. This route was chosen to
783 help attenuate contextual overlap between time and space (see methods for details). b) Example pictures of the campus
784 areas where the experiment took place. c) A visual representation of each trial as shown on the tablet screen. After the
785 experimenter tapped the screen, a word was displayed following a variable fixation window. Participants were then shown
786 to the next location (black dot in (a)) and the process was repeated.

787

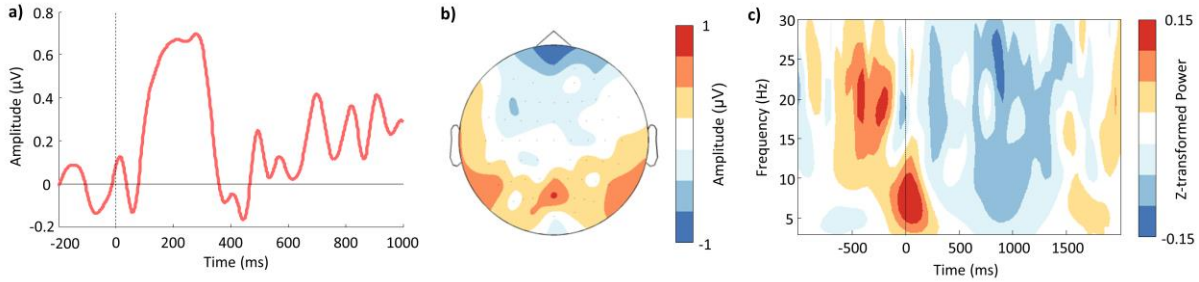

788

789 Figure 2. 'Real world' EEG data. a) The P300 component elicited over parietal channels (P1, Pz, P2, PO3, POz, PO4),
790 averaged across all trials in response to stimulus onset. Only independent components explaining eye-blinks, saccades and
791 other muscular artifacts have been removed from the data. b) Topography of time-locked data, 0 to 400ms post-stimulus.
792 c) Time-frequency plot depicting oscillatory activity across all trials and all channels locked to stimulus onset.

793

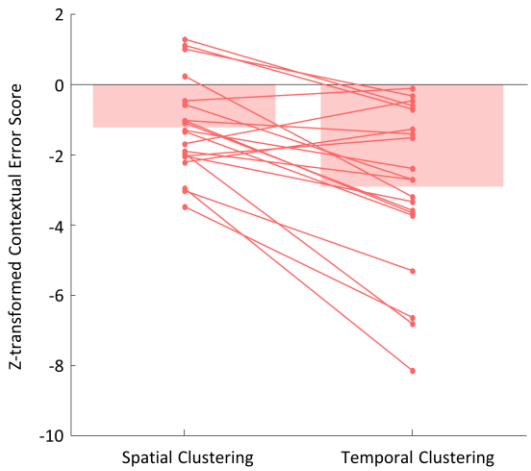

Figure 3. Bar plot representing the mean spatial and temporal 'z-transformed contextual error score'. Zero indicates the contextual error expected by chance. A score less than zero indicates less contextual error than expected by chance, and therefore greater contextual clustering. Individual scatter points represent the mean contextual error score of each participant. Spatial and temporal clustering was significantly greater than chance ($p<0.001$). Temporal was significantly greater than spatial clustering ($p<0.001$).

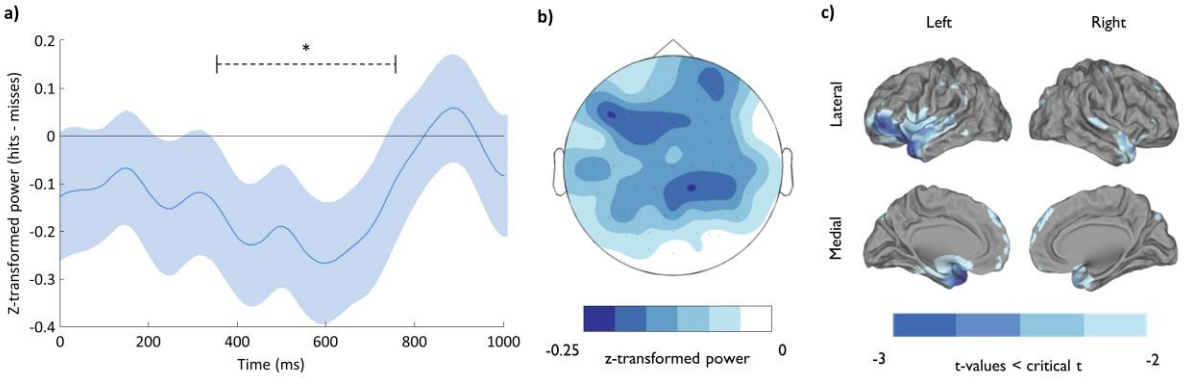

Figure 4. Subsequent memory effect (hits minus misses) in the a priori region of interest (0 to 1000ms, 15 to 20Hz, all channels). a) The time course of z-transformed power differences between the later remembered (hits) and later forgotten (misses) items, averaged over all channels and frequency bins with standard error of the mean. b) Topography of significant power differences between hits and misses, averaged across the a priori time-frequency window. c) Source localisation of a priori window of interest. Differences show a significantly greater beta power decrease in the hits condition over left inferior frontal regions.

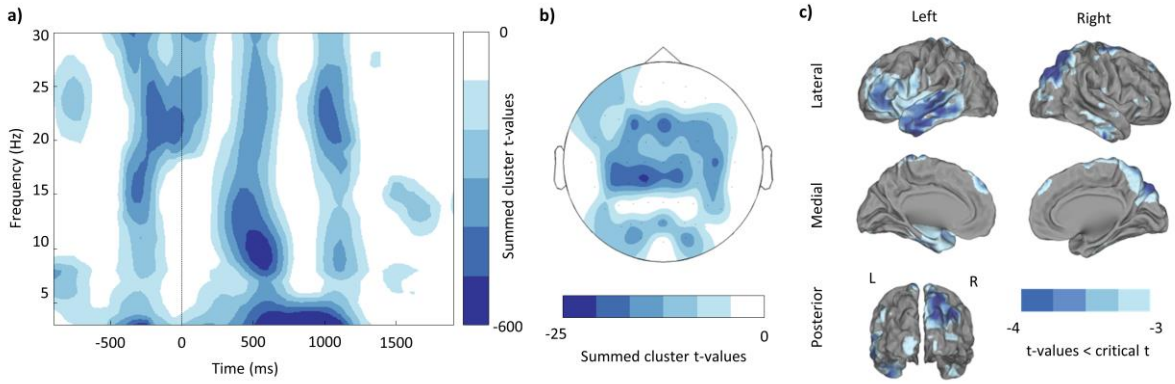

Figure 5. Subsequent memory effect (hits – misses) across low and mid-frequencies. a) Time-frequency representation of cluster t-values for each significant sliding window. All non-significant FDR corrected time-frequency windows are masked. b) Topography of significant difference between hits and misses for theta (3-4Hz, 600ms to 1200ms post-stimulus). c) Source localisation of the significant theta effect.

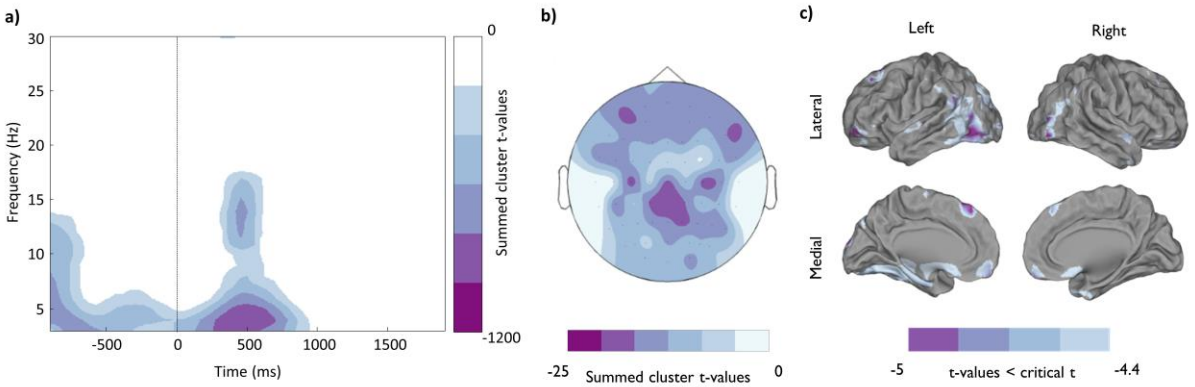

Figure 6. Neural correlates of spatial clustering. a) Time-frequency representation of cluster summed t-values for windows where the observed correlation coefficient was significantly different from the null hypothesis (i.e. r = 0). b) Topography of the post-stimulus theta power decrease associated with greater spatial clustering (3 – 4Hz, -1000 to 1000ms). c) Source reconstruction of the same theta power decrease accompanying greater spatial clustering.

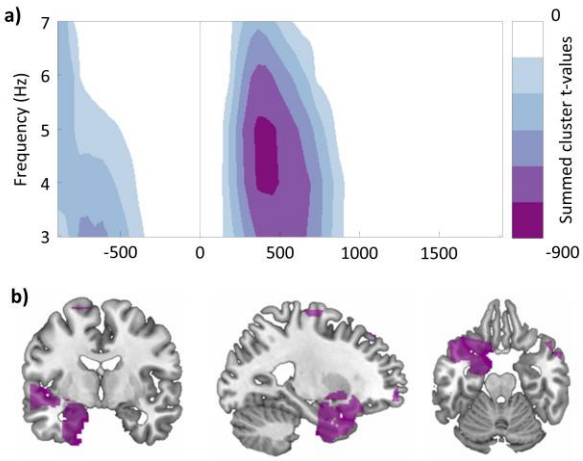

Figure 7. Significant decreases in theta power activity for spatial clustering in comparison to temporal clustering. a) Sensor level time-frequency representation of significant differences in theta power. b) Orthographic plot of source activity differences between spatial clustering and temporal clustering,